International Journal of Solids and Structures xxx (2015) xxx–xxx

Contents lists available at ScienceDirect

International Journal of Solids and Structures

journal homepage: www.elsevier.com/locate/ijsolstr

Revisiting the identification of generalized Maxwell models from experimental results

D. Jalocha [a,b,*], A. Constantinescu [a], R. Neviere [b]

[a] Laboratoire de Mecanique des Solides, CNRS UMR 7649, École Polytechnique, ParisTech, 91128 Palaiseau Cedex, France
[b] Herakles, Centre de Recherche du Bouchet, 9 rue Lavoisier, 91710 Vert Le Petit, France

ARTICLE INFO

Article history:
Received 18 June 2014
Received in revised form 6 February 2015
Available online xxxx

Keywords:
Maxwell model
Identification
Relaxation time
Relaxation modulus
Complex modulus

ABSTRACT

Linear viscoelastic material behavior is often modeled using a generalized Maxwell model. The material parameters, i.e. relaxation times and elastic moduli, of the Maxwell elements are determined from either a *relaxation* or a *Dynamical Mechanical Analysis* (DMA) experiments. The underlying mathematical problem is known to be ill-posed, which means that uniqueness of the identification is not assured and that small errors in the initial data will conduct to high discrepancies in the identified parameters. The standard technique to remove the ill-posedness is to chose a priori a series of relaxation times and to identify only the moduli. The aim of this paper is to propose two techniques to identify an optimal series of relaxation times. In the case of the relaxation experiment relaxation times will be optimized from the numerical integration of the measured relaxation spectrum. In the case of the DMA experiments we show that mathematical results obtained by Krein and Nudelmann can be used to determine the complete series of relaxation times. The methods are illustrated by identification examples using both artificial and experimental data. The results show that the methods provide a good match of the identified models in term of relaxation or complex moduli.

1. Introduction

A large number of materials including rubber, polymers, composites, concrete, etc. have a viscoelastic mechanical behavior which is often represented using a generalized Maxwell model (Findley et al., 1976). The model presents several merits: it is simple, robust and can be identified from *relaxation* or *Dynamical Mechanical Analysis* (DMA) experiments. Moreover it can cover a large range of characteristic times in both experiments. Application of the generalized Maxwell model cover different classes of polymers amorphous or cross-linked polymers (Brinson, 2008), polydisperse, high density polyethylene (Otegui et al., 2013) etc. Other applications cover concrete materials as in Park and Kim (2001).

Further extension based on the Linear generalized Maxwell model are cover nonlinear viscoelastic material behaviors, where different parameters like the elastic moduli or the relaxation times will further depend on different parameters. Let us cite, the curing dependent relaxation moduli proposed in Zarrelli et al. for epoxy materials or a prestrain dependent complex modulus proposed for propellant in Thorin et al. (2013,).

The identification of the relaxation spectrum of a viscoelastic system, corresponds to the determination of the relaxation kernel in an integral equation and is denoted as a Fredholm integral equation of the first kind. The problem has attracted a lot of attentions during the last decades due to its inherent difficulties. It is mathematically ill-posed, implying that the identification of the kernel is not uniquely assured and that small errors in the initial data will conduct to high discrepancies in the identified kernel. Within the recent mathematical literature, we can cite the work of Grasselli (1994), Janno and Von Wolfersdorf (1997), Von Wolfersdorf (1993), Cavaterra and Grasselli (1997), which recovered the relaxation spectrum by reducing the problem to a nonlinear Volterra integral equation using a Fourier method to solve the direct problem and by applying the contraction principle. Further results reveled that the problem can also be solved in a heterogeneous medium, as in Lorenzi (1999), Lorenzi and Romanov (2006) or recently de Buhanand and Osses (2010) meaning that a spatial material heterogeneity can also be recovered if specific conditions are satisfied.

* Corresponding author at: Laboratoire de Mecanique des Solides, CNRS UMR 7649, École Polytechnique, ParisTech, 91128 Palaiseau Cedex, France.
E-mail addresses: jalocha@lms.polytechnique.fr (D. Jalocha), andrei.constantinescu@lms.polytechnique.fr (A. Constantinescu), robert.neviere@herakles.com (R. Neviere).

http://dx.doi.org/10.1016/j.ijsolstr.2015.04.018

In order to eliminate the ill-posedness of the identification problem, a standard technique consists of defining a priori the characteristic times for the Prony's series and pursuing the identification only for the elastic moduli of the different elements. This technique is described for example in Honerkamp (1989), Honerkamp and Weese (1990) for the DMA experiments, where the identification is performed on the complex moduli of the material. A recent application example is given in Diani et al. (2012), where a generalized Maxwell model is identified to describe the viscoelastic behavior of shape memory polymers. For the relaxation experiment a dual method is proposed in Baumgaertel and Winter (1992), Gerlach and Matzenmiller (2005) where the relaxation modulus is identified. Other techniques are based on different numerical schemes to tackle this problem, as for example the combination of Laplace transform and Padé approximants reported in Carrot and Verney (1996), or the cumulative relaxation spectrum proposed in Xiao et al. (2013).

The aim of this paper is to improve the existing techniques by proposing a novel way to determine a series of characteristic times. In the case of a DMA experiment, the improvement is based on a mathematical result given by Krein and Nudelman (1998), which permits to identify the relaxation times as the zeros of two complex functions constructed from the measured data. This problem setting does not eliminate the ill-posedness of the initial problem. Two algorithmic matrices have to be positive definite in order to numerically solve the problem and this is realized through a regularization technique. However this imposes more natural restrictions in the problem when compared with an artificial set of characteristic times. In the case of the relaxation experiments, the idea is to optimize the a priori set of relaxation time by imposing a closer representation of the relaxation function by reanalyzing the Riemann integration process. Results for both experiments provide a smaller number of branches in the generalized Maxwell model than traditional methods and keep the quality of the representation.

The paper starts with an overview of the viscoelastic generalized Maxwell model where notations and general concepts are introduced, as the continuous spectrum or the discrete Prony's series. The third section presents the standard identification technique of parameters from DMA experiments as presented by Honerkamp (1989), Honerkamp and Weese (1990) and the theoretical results of Krein and Nudelman (1998) as well as the proposed identification algorithm. The discussion continues with the identification method of parameters from relaxation test as proposed in Baumgaertel and Winter (1992), Gerlach and Matzenmiller (2005) and the proposed optimal identification of relaxation times. The two methods are illustrated in the last chapter by a series of examples: first using artificial data, which also permits to investigate the influence of the noise and second using experimental data from literature and measurements.

2. Viscoelasticity and Prony's series

Let us start by recalling some concepts in linear viscoelasticity in order to define the notations and the basic equations used in this study.

The viscoelastic constitutive behavior can be represented in the time domain, according to Markovitz and Hershel (1977), by relating histories of stresses, σ, and strains, ε, through the integral equation:

$$\sigma(t) = \int_{-\infty}^{t} E(t-\tau)\frac{d\varepsilon(\tau)}{d\tau}d\tau \tag{1}$$

where E denotes the relaxation kernel.

The dual representation of constitutive equation in the frequency domain, relates the Fourier transform of stress and strains, denoted as σ^* and ε^* respectively, by a linear equation:

$$\sigma^*(\omega) = E^*(\omega)\varepsilon^*(\omega) \tag{2}$$

$E^*(\omega)$ is the complex modulus depending of the frequency ω and obtain through the same Fourier transform as stresses or strains.

The two equations in the time domain or frequency domain, are equivalent and can be obtained the a direct or inverse Fourier Transform denoted with a $*$.

The main constitutive unknown is the relaxation spectrum $H(\tau)$ (Findley et al., 1976) which is related to the relaxation modulus $E(t)$ by:

$$E(t) = E_0 + \int_{-\infty}^{\infty} H(\tau)e^{-\frac{t}{\tau}}d\ \ln(\tau) \tag{3}$$

and to the dynamical modulus $E^*(\omega) = E'(\omega) + iE''(\omega)$ by:

$$\begin{aligned} E'(\omega) &= E_0 + \int_{-\infty}^{\infty} H(\tau)\frac{\omega^2\tau^2}{1+\omega^2\tau^2}d\ \ln(\tau) \quad E^{Prime}(\omega) \\ &= \int_{-\infty}^{\infty} H(\tau)\frac{\omega\tau}{1+\omega^2\tau^2}d\ \ln(\tau) \end{aligned} \tag{4}$$

For practical reasons it is convenient to use a model, where the continuous spectrum of relaxation $H(\tau)$ is replaced with a finite spectrum $\hat{H}(\tau)$ (Eq. (5)). This later is interpreted as simple rheological elements, springs and dampers, and is denoted generalized Maxwell model (see Fig. 1). It mathematical description is the finite Prony's series (τ_i, E_i) and the spectrum becomes:

$$\hat{H}(\tau) = \sum_{i=1}^{n} E_i\ \delta\left(1-\frac{\tau}{\tau_i}\right) \tag{5}$$

where δ is the Dirac function. The relaxation time τ_i associated to the element i is related to the characteristic time of the spring-damper element, and is defined as the ratio of the viscosity over the elastic moduli, i.e. $\tau_i = \frac{\eta_i}{E_i}$.

This representation is often used in finite element models, see Simo and Hughes (2008) for the time integration within a finite element code.

In the discrete case of Prony series, the relaxation modulus $E(t)$ is represented as:

$$E(t) = E_0 + \sum_{i=1}^{n} E_i\ e^{-\frac{t}{\tau_i}} \tag{6}$$

where E_0 represents the stiffness of the model at large times and n denotes the number of branches of the generalized Maxwell model. In the frequency domain, the dynamical modulus $E^*(\omega)$ becomes:

$$E'(\omega) = E_0 + \sum_{i=1}^{n}\frac{E_i\ \omega^2\tau_i^2}{1+\omega^2\tau_i^2} \quad E''(\omega) = \sum_{i=1}^{n}\frac{E_i\ \omega\tau_i}{1+\omega^2\tau_i^2} \tag{7}$$

Let us now consider that mechanical experiments such as relaxation test or cyclic loading test using a Dynamical Mechanical Analyzer (DMA) provide a data series representing a continuous

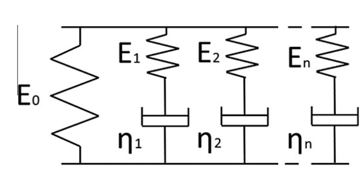

Fig. 1. A schematic representation of the generalized Maxwell model as a parallel association of n Maxwell units, i.e. linear spring and damper (E_i, τ_i) and a linear spring of stiffness E_0.

Please cite this article in press as: Jalocha, D., et al. Revisiting the identification of generalized Maxwell models from experimental results. Int. J. Solids Struct. (2015), http://dx.doi.org/10.1016/j.ijsolstr.2015.04.018

spectrum of relaxation times. The practical question is that of the identification of an optimal discrete model from this data. This question is essentially the identification problem of the generalized Maxwell model, i.e. determining the finite Prony's series $\{(\tau_i, E_i);\ i = 1, n\}$ from the measured data.

From a mathematical point of view, it corresponds to the identification of the kernel of an integral Fredholm equation and it is well known that these identification problems are ill-posed (Lavrentiev, 1967), more precisely uniqueness of solutions is not assured and the identification is instable, i.e. a small errors in the data as generate by noise will develop a large error into the identified output (Hansen, 1992).

3. DMA experiment

The loading during DMA experiments is a sinusoidal strain $\varepsilon = \varepsilon_0 \, sin(\omega t)$, which is associated to the real part of the complex strain $\varepsilon^* = \varepsilon_0 \, e^{i\,\omega t}$. After a short transient period a stable strain–stress loop occurs and the stress response can equally be expressed in a sinusoidal form, $\sigma = \sigma_0 \, sin(\omega t + \delta)$, associated to the real part complex stress $\sigma^* = \sigma_0 \, e^{i(\omega t + \delta)}$. For a given frequency ω, the complex dynamical modulus is defined as

$$E^*(\omega) = \frac{\sigma^*}{\varepsilon^*} = E'(\omega) + iE''(\omega)$$

If the measurement is repeated for m different frequencies $\omega_i,\ i = 1, m,$ the preceding procedure will provide data set $(\omega_j, E'_j(\omega_j), E''_j(\omega_j))$ for $1 \leqslant j \leqslant m$.

3.1. Existing identification procedure: the HW method

Different identification methods for the material parameters of the generalized Maxwell model have been proposed in the past, see for example the general discussion in Gerlach and Matzenmiller (2005).

The method discussed next is a development based on the method proposed by Honerkamp (1989) and Honerkamp and Weese (1990), denoted here as the *HW method*.

Let us consider the experimental data set formed by m triplets (ω_j, E'_j, E''_j), with $j = 1,\ m$. The problem is to identify a corresponding Prony's series, defined by $2n$ parameters $(E_i,\ \tau_i)$, with $i = 1, n$, of a generalized Maxwell model.

The HW method can be resumed in the following steps:

- **Step 1:** *Chose arbitrarily the number of n elements and the corresponding values of the relaxation time of each element τ_i.*
  This is a regularization step it as it eliminates one of the major unknowns. It further transforms (7) into a linear equation for the unknown parameters E_i defined by:

$$\mathbf{E}' = \mathbf{E_0} + \mathbf{AE} \quad and \quad \mathbf{E}'' = \mathbf{BE} \tag{8}$$

where: $\mathbf{E}'$, $\mathbf{E}''$, $\mathbf{E_0}$, $\mathbf{E}$ are the vectors of the different moduli respectively. The matrix $\mathbf{A}$ and $\mathbf{B}$ are defined as:

$$\mathbf{A} = (a_{ij}) \quad a_{ji} = \frac{\omega_j^2 \tau_i^2}{1 + \omega_j^2 \tau_i^2}$$

and

$$\mathbf{B} = (b_{ij}) \quad b_{ji} = \frac{\omega_j \tau_i}{1 + \omega_j^2 \tau_i^2}$$

- **Step 2:** *Solve (8) in a least square sense*
  The vector of moduli $\mathbf{E}$ is realizes the following least squares minima:

$$\mathbf{E} = \underset{\mathbf{d}}{\mathrm{ArgMin}} \frac{1}{2} \|(\mathbf{E}' - \mathbf{E_0}) - \mathbf{Ad}\|^2 \quad \text{and/or}$$
$$\mathbf{E} = \underset{\mathbf{d}}{\mathrm{ArgMin}} \frac{1}{2} \|\mathbf{E}'' - \mathbf{Bd}\|^2 \tag{9}$$

The solution is obtained using the pseudo-inverse or the Moore–Penrose inverse matrix, denoted by $^+$ (see for details for example Press et al.) and the solution is written as:

$$\mathbf{E} = \mathbf{A}^+(\mathbf{E}' - \mathbf{E_0}) \ or \ \mathbf{E} = \mathbf{B}^+\mathbf{E}'' \tag{10}$$

More precisely, $\mathbf{A}^+ = \mathbf{U_A}\Sigma_\mathbf{A}^{-1}\mathbf{V_A}$, where $\mathbf{A} = \mathbf{V_A}\Sigma_\mathbf{A}\mathbf{U_A^T}$ is the singular value decomposition of the matrix $\mathbf{A}$. As the preceding linear systems can still be ill-posed one can use different regularization techniques to stabilize the solution of such a system, see discussed in Hansen (1992).

3.2. Proposed procedure: the KN + HW method

The method proposed next permits to replace the arbitrary choice of the relaxation times with an exact computation of the series of relaxation times. This novelty eliminates the first step of the *HW* method, where the relaxation times are generally imposed as a linear series on the logarithmic scale.

The technique discussed is based on the mathematical result in complex analysis obtained by Krein and Nudelman (KN) and presented in Krein and Nudelman (1998). The modified method will be further denoted as *KN + HW method*.

The Krein and Nudelamn result has recently been applied for the identification of a viscoelastic materials from measurements in a split Hopkinson bar experiment (Collet et al., 2013).

In order to introduce the technique, we shall first present a series of mathematical notations and results. The Nevanlinna Pick interpolation problem (see for example Byrnes and Lindquist (2000)) consists in finding a complex function $F : \mathbb{C} \longrightarrow \mathbb{C}$ interpolating the data pairs $(z_k, c_k)_{k=1,m}$, i.e.:

$$F(z_k) = c_k \quad k = 1, m \tag{11}$$

Moreover, a function $F(z)$ will be denoted as a *S-function* if:

$$F(z) = \gamma + \int_0^\infty \frac{d\sigma(t)}{t - z} \tag{12}$$

where $0 \leqslant \gamma$ and $0 \leqslant d\sigma(t)$. The result of Krein and Nudelman (see Krein and Nudelman (1998) Section 4) states that if $z_k \in \mathbb{C}^+,\ k = 1, m,$ then the interpolation problem has a solution in the class of S-functions if and only if the quadratic forms defined by the matrices:

$$M^1_{kj} = \frac{c_j - \overline{c_k}}{z_j - \overline{z_k}} \quad M^2_{kl} = \frac{z_j c_j - \overline{z_k c_k}}{z_j - \overline{z_k}} \tag{13}$$

are positive definite, i.e.:

$$0 \leqslant \zeta \ M^1 \ \overline{\zeta} \ and \ 0 \leqslant \zeta \ M^2 \ \overline{\zeta} \quad \forall \zeta \in \mathbb{C} \tag{14}$$

and that the problem has a unique solution if at least one of the two forms degenerates.

Let us show next that the viscoelastic identification problem can be transformed in the structure defined by the Pick–Nevalinna interpolation problem in the class of S-function.

As a first remark, let us observe that the complex modulus of the viscoelastic problem is the conformal transform of an *S-function*. Starting from Eq. (4), it can be expressed as:

$$E^*(\omega) = E_0 + \int_0^\infty H(\tau) \frac{i\omega \ \tau}{1 + i\omega \ \tau} d\tau \tag{15}$$

Please cite this article in press as: Jalocha, D., et al. Revisiting the identification of generalized Maxwell models from experimental results. Int. J. Solids Struct. (2015), http://dx.doi.org/10.1016/j.ijsolstr.2015.04.018

After the change of variable $s = \frac{1}{\tau}$, the complex modulus is rewritten as a function of the reduced spectrum $h(s) = \frac{H(\frac{1}{\tau})}{\tau}$ as:

$$E^*(\omega) = E_0 + \int_0^\infty \frac{h(s)}{s + i\omega} ds \tag{16}$$

Considering the new following change of variable:

$$p(z) = \frac{E^*(iz)}{z} \tag{17}$$

Eq. (16) becomes:

$$p(z) = \int_0^\infty \frac{g(s)}{s - z} ds \tag{18}$$

with:

$$g(s) = \left(E_0 + \int_0^\infty \frac{h(u)}{u} du \right) \delta(s) + \frac{h(s)}{s} \tag{19}$$

This also shows that the function $p(z)$ of (18) is a S-function.

As a second remark, let us analyze in the particular case of a generalized Maxwell model the degeneracy of the quadratic forms defined by M^1 and M^2, see Eq. (13). Starting from (17), one can show that both forms can be expressed as:

$$M^1_{kl} = i\frac{\overline{E^*_k} - E^*_l}{\omega_k + \omega_l} = \int_0^\infty h(s) \frac{ds}{(s - i\omega_k)(s + i\omega_l)} \tag{20}$$

and

$$M^2_{kl} = \frac{\frac{\overline{E^*_k}}{\omega_k} + \frac{E^*_l}{\omega_l}}{\omega_k + \omega_l} = \frac{E^*(0)}{\omega_k\omega_l} \int_0^\infty \frac{h(s)}{s} \frac{ds}{(s - i\omega_k)(s + i\omega_l)} \tag{21}$$

where $E^*_k = E^*(\omega_k)$ for $k = 1,\ m$,

Let us further denote by v and w the eigenvectors of the kernels of the matrices M^1 and M^2, respectively. They are associated with the 0 eigenvalue which implies that:

$$v \cdot M^1 \cdot \overline{v} = 0$$

Taking into account Eq. (20), the last equation also writes:

$$\int_0^\infty \left(h(s) \left\| \sum_{k=1}^m \frac{v_k}{(s - i\omega_k)} \right\|^2 \right) ds = 0 \tag{22}$$

In the case of a generalized Maxwell model, $h(s) = \sum_i \delta(s - s_i)$ and the equality (22) is verified only if the points $(s_i)_{i=1,n}$ are the zeros of the rational function:

$$f_1(s) = \sum_{k=1}^m \frac{v_k}{(s - i\omega_k)} \tag{23}$$

A similar reasoning on the matrix M^2 implies that the points $(s_i)_{i=1,n}$ are also the zeros of a second rational function:

$$f_2(s) = \sum_{k=1}^m \frac{w_k}{(s - i\omega_k)} \tag{24}$$

The relaxation times are therefore obtained as $\tau_i = \frac{1}{s_i}$, the inverse values of the common zeros of the functions f_1 and f_2.

Finally, the *KN + HW method* is summarized as follows:

- **Step 1:** *Build the two complex matrices* $\mathbf{M^1}$ *and* $\mathbf{M^2}$ defined by their components:

$$M^1_{kl} = i\frac{\overline{E^*_k} - E^*_l}{\omega_k + \omega_l} \quad M^2_{kl} = \frac{\frac{\overline{E^*_k}}{\omega_k} + \frac{E^*_l}{\omega_l}}{\omega_k + \omega_l} \tag{25}$$

where $E^*_k = E'_k + iE''_k$ with $k,\ l = 1,\ m$ and $\overline{E^*_k}$ the conjugate complex number of E^*_k.

- **Step 2:** *Check the positive definition of matrices* $\mathbf{M^1}(E^*, \omega)$ *and* $\mathbf{M^2}(E^*, \omega)$.
  If the generalized Maxwell model is accepted to represent the measurements, noise is one of the reason for the failure of positive definiteness. In this case we can filter the data and obtain corrected positive defined matrices. The filtering proposed here is different from the correction in Collet et al. (2013). According to Gu et al. (1993) and Greene and Krantz (1997), $\mathbf{M^1}$ and $\mathbf{M^2}$ are positive semi definite matrices if E^* is holomorphic. A possible correction is therefore given by the correction obtained by the least square fit of a holomorphic function, for example of a rational polynomial P, to the data E^*_k. Matrices $\mathbf{M^1}$ and $\mathbf{M^2}$ are then build after using the corrected data $P(\omega_k)$ and not the measured data E^*_k.
- **Step 3:** *Compute the* $\mathbf{v}$ *and* $\mathbf{w}$ *the eigenvectors spanning the kernel of* $\mathbf{M^1}$ $\mathbf{M^2}$, *respectively and the two complex-valued functions* f_1 *and* f_2:

$$f_1(s) = \sum_{j=1}^m \frac{v_j}{s + i\omega_j} \quad f_2(s) = \sum_{j=1}^m \frac{w_j}{s + i\omega_j} \tag{26}$$

- **Step 4:** *Find numerically the common real positive zeros* s_i *of* f_1 *and* f_2.
  The number of solutions will define the number of elements in the generalized Maxwell model and the values of the characteristic times are:

$$\tau_i = \frac{1}{s_i} \tag{27}$$

- **Step 5:** *Compute the values of the moduli*, by using the *HW* inverse identification described before.

4. Relaxation experiments

The loading during a relaxation experiment, consist in impose a deformation step to the material sample: $\varepsilon(t) = \varepsilon_0\ H_e(t)$, where $H_e(t)$ denotes the Heaviside function, and record the continuously decreasing stress history $\sigma(t)$. The relaxation modulus is defined as

$$E(t) = \frac{\sigma(t)}{\varepsilon_0}$$

As a consequence, the experimental data representing the continuous relaxation spectrum is a set of m time-modulus pairs: $(t_j, E_j(t))$ with $j = 1,\ m$.

4.1. Existing procedure: the B method

The method developed in this section to identify the generalized Maxwell model from the continuous relaxation time spectrum is based on the standard method proposed and described by Baumgaertel in Baumgaertel and Winter (1992). It will be denoted here for simplicity as *B method*.

Let us recall that the evolution of the relaxation modulus is a function of time and can be modeled by the following expression (see for example Smith (1971) for further details):

$$E(t) = E_0 + \frac{E_g - E_0}{\left(1 + \frac{t}{t_0}\right)^\beta} \tag{28}$$

where E_0 and E_g denote the value of the relaxation modulus at long and short times respectively. t_0 and β are parameters determined by fitting the measured data: $(t_j, E_j(t))$.

Using the change of variable $f(z) = \frac{H(\frac{1}{z})}{z}$, Eq. (3) becomes:

$$E(t) - E_0 = \int_{-\infty}^{\infty} H(\tau)\ e^{-\frac{t}{\tau}} d\ln(\tau) = \int_{0}^{\infty} f(z) e^{-tz} dz \tag{29}$$

Eq. (29) further implies that the relaxation modulus is the Laplace transform of the function $f(z)$ (see for example Widder (1946)):

$$E(t) - E_0 = \mathcal{L}(f(z)) \tag{30}$$

The relaxation time spectrum is obtained as the inverse Laplace transform of the expressions in Eq. (28):

$$H(\tau) = \frac{(E_g - E_0)}{\Gamma(\beta)} \left(\frac{\tau}{t_0}\right)^{-\beta} e^{-\frac{t_0}{\tau}} \tag{31}$$

With $\Gamma(\beta)$ the Gamma function of β.

The shape of the relaxation time spectrum is now a concave function with a peak H_{max} reaching at its maximum in $\tau_{max} = \frac{t_0}{\beta}$, i.e. $H(\tau_{max}) = H_{max}$.

The question defined next is the identification of the discrete generalized Maxwell model associated with this relaxation spectrum. The discrete relaxation spectrum $\hat{H}(\tau)$ corresponds to a staircase function and represents an approximation of the continuous spectrum $H(\tau)$, see Eq. (5). As in the frequency domain, the standard practice is to chose a priori the set of time instants τ_i placed at equal distance on the logarithmic scale, see Baumgaertel and Winter (1992).

Let us note $\tau_i^+ = \sqrt{\tau_i \tau_{i+1}}$ and $\tau_i^- = \sqrt{\tau_i \tau_{i-1}}$, the geometric average of the intervals (τ_{i+1}, τ_i) and (τ_i, τ_{i-1}) on the logarithm scale, respectively. The direct combination of Eqs. (29) and (6) under the assumption of a constant function of value $H(\tau_i)\ e^{-\frac{t}{\tau_i}}$ over each interval (τ_i^-, τ_i^+), conducts after some simple calculations to the expression:

$$E_i e^{-\frac{t}{\tau_i}} = \int_{\tau_i^-}^{\tau_i^+} H(\tau) e^{-\frac{t}{\tau}}\ d\ln(\tau) \approx\ H(\tau_i)\ e^{-\frac{t}{\tau_i}} \ln\left(\sqrt{\frac{\tau_{i+1}}{\tau_{i-1}}}\right) \tag{32}$$

The identification procedure is now reduced to the determination of the values of the moduli $E_i = H(\tau_i)\ \ln(r_i)$, where $r_i = \sqrt{\frac{\tau_{i+1}}{\tau_{i-1}}}$.

4.2. Proposed procedure: the R method

The logarithm equidistant distribution of relaxation times proposed before does not necessary provide the most accurate approximation of the relaxation spectrum. The alternative method proposed here and denoted next as the *R method* will directly optimize the distance between the discrete and the continuous relaxation spectrum. The discrete relaxation spectrum $\hat{H}(\tau)$ becomes a staircase function of variable width. For a general discussion of similar methods, the approximation of functions minimizing integral norms is presented for example in Kurtz et al. (2004).

Let us now define the approximate support of the relaxation spectrum defined as the interval on the time axis where it is non-zero. More precisely, the support is defined in terms of the maximal value of the spectrum, as the interval where $H(\tau) \geqslant c_1 H_{max}$. The c_1 is an arbitrary parameter and was chosen in the range $0.001 \leqslant c_1 \leqslant 0.05$. The support will be denoted as (τ_{c1}, τ_{c2}).

The staircase function $S(\tau)$, representing the generalized Maxwell model with n elements (see Fig. 2) is defined as:

$$S(\tau) = \sum_{i=1}^{n} H(\tau_i) U_{(t_{i-1}, t_i)}(\tau) \tag{33}$$

where $\tau_i = \frac{t_{i-1}+t_i}{2}$ and the unit box function is defined as

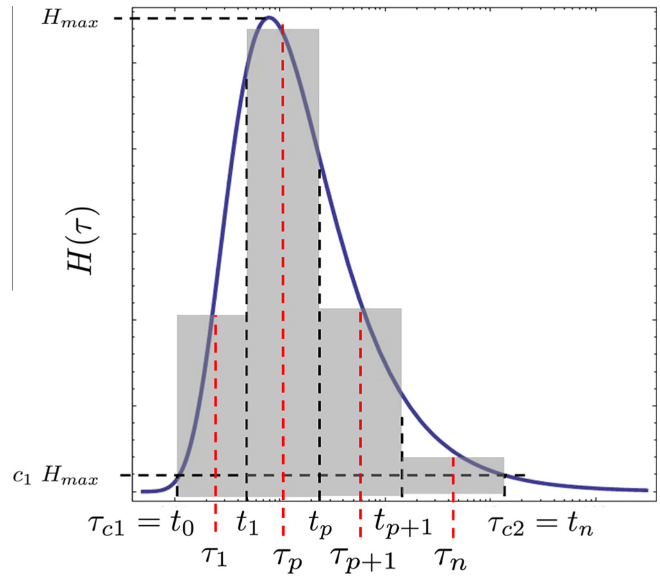

Fig. 2. Example of continuous relaxation time spectrum $H(\tau)$ and a staircase function $S(\tau)$. Computation principle of τ_i.

$$U(t_{i-1}, t_i) = \begin{cases} 1 \text{ if } t_{i-1} \leqslant \tau \leqslant t_i \\ 0 \text{ otherwise} \end{cases}$$

The closed-form expression of $H(\tau)$, given in Eq. (31), permits to compute the closed-form expression of the integral of the continuous relaxation spectrum. Moreover, let us denote R, the residual function measuring the relative distance between $H(\tau)$ and $S(\tau)$:

$$R = \frac{\left\| \int_{\tau_{c1}}^{\tau_{c2}} H(\tau) - S(\tau) d\tau \right\|}{\left\| \int_{\tau_{c1}}^{\tau_{c2}} H(\tau) d\tau \right\|} \tag{34}$$

The optimal finite distribution of relaxation times in the support of the spectrum is now obtained for a fixed number of elements n by minimizing the residual R. The time instants (t_i), $i = 1,\ n+1$, defining the partition of the support in n elements with $t_0 = \tau_{c1}$ and $t_n = \tau_{c2}$, are related to the relaxation times by $\tau_i = \frac{t_{i-1}+t_i}{2}$ with $i = 1,\ n$. A schematic representation of the continuous spectrum and the staircase approximation is displayed in Fig. 2.

The optimization procedure has been programmed using standard *Mathematica* commands (Wolfram Research, 2014) with a required precision of 1% on the position of the partition points.

5. Application to artificial data

As a first application we shall apply the preceding methods to the identification of a Maxwell model using artificial data, obtained through numerical simulation of the experiments from a predefined generalized Maxwell model. This step permits to asses the robustness of the methods and investigate the influence of the artificial noise on the accuracy of the identification.

Let us now examine a viscoelastic behavior generated with a four elements generalized Maxwell model ($n = 4$) defined by the values of relaxation times and elastic moduli given in Table 1. Modulus value at infinite time is taken equal to zero ($E_0 = 0$).

Table 1
Generalized Maxwell model used to generate artificial data.

τ_i (s)	0.05	0.2	2	10
E_i (Pa)	400	300	150	8

The relaxation modulus and the complex modulus are artificially generated by direct computation using Eq. (6) and perturbed by a white noise of 5% or 10%. The perturbed data in the case of 5% noise are displayed in Fig. 3.

5.1. Parameter identification using the complex modulus

Let us first identify the model from the artificial complex modulus and compare the results obtained from the HW and KN + HW methods.

As stated in the presentation of the KN + HW method, the key point of the identification algorithm is the positive definition of the two matrices $\mathbf{M^1}$ and $\mathbf{M^2}$ and the necessary correction of the data.

The positive definiteness of the matrixes is improved after replacing the initial noisy data (ω_i, E'_i, E''_i) with "corrected" data $(\omega_i, E'^c_i, E''^c_i)$ obtained after fitting with a rational polynomial P defined as:

$$E'^c_i + iE''^c_i = \sum_{i=1}^{5} \frac{a_i\ \omega_i^2 + i\ b_i\ \omega_i}{c_i + \omega_i^2} \tag{35}$$

The values of the coefficients of P obtained from the least square fitting procedure are presented in Table 2.

Table 2
The coefficients of the rational polynomial P used in the data correction.

a_i	8.3	157.5	290.2	419.9	6.9
b_i	−3.8	71.8	1367.8	8506.6	−374.5
c_i	0.2	0.3	22.2	410.2	2866.8

In order to illustrate the effect of the "correction" procedure on the positive definition of the matrices $\mathbf{M^1}$ and $\mathbf{M^2}$ we have displayed the evolution of the eigenvalues on Fig. 4. The plot displays the eigenvalues with abscissa the number of the eigenvalue and the logarithm of its norm as ordinate. The color code display blue and red for positive and negative eigenvalue respectively. The example show that the correction process does not solve the problem of the positive definition of the matrices as negative eigenvalue are still present after the correction, however one can remark that the first negative eigenvalue at now at least several order of magnitudes lower and that the very small eigenvalues characterizing the kernel are now clearly isolated. The graphical comparison between the initial and the "corrected" data is displayed in Fig. 5 shows that the process brings only a smoothing in the identification process. However the real impact of the smoothing will be observed in the next step: the determination of the common positive zeros of the complex functions f_1 and f_2.

The evolution of absolute values of $\|f_1\|$ (blue line) and $\|f_2\|$ (red line) as function of s in a double logarithmic plot is displayed in Figs. 6–8 for the initial unperturbed data, the corrected data in the case of 5% and 10% noise respectively.

The functions computed for initial unperturbed data, see Fig. 6, show that zeros of the function have to be understood in a numerical sense, even in this case. The zero value represents only a $\approx 10^{-4}$ for one of the elements and goes down to $\approx 10^{-10}$ for the most pronounced zero. The zeros values are positioned at $s_i = 1/\tau_i$ as expected.

Concerning the case of noisy data, one can remark that in Figs. 7(a) and 8(a), corresponding to the uncorrected noisy data, only one out of the four common zeros of f_1 and f_2 is recognizable. However, the functions computed from the corrected data display very clearly three out of four common zeros in Figs. 7(b) and 8(b). Moreover, the identified values of relaxation times, see Table 3, present only a small shift in spite of the noise in the data. One can further remark that the Krein and Nudelmann result will find one relaxation time per decade, without respecting a linear distribution in the logarithmic scale.

The relaxation times τ_i, from the common zeros can now be used in the identification of the moduli E_i from Eq. (8). The generalized Maxwell model is now completely determined and the values of the material parameters are presented in Table 3.

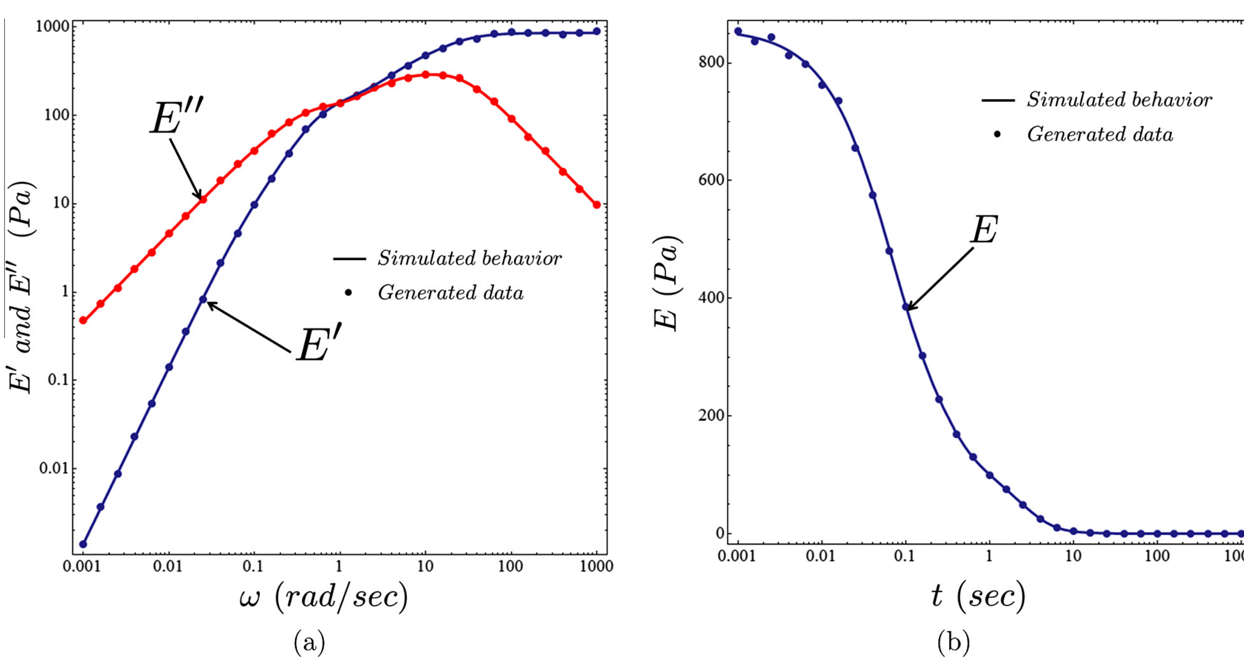

Fig. 3. Artificial experimental data: (a) real (E') and imaginary (E'') part of the complex modulus (E^*) and (b) relaxation modulus (E). The continuous line represents the initial noise-free data and the dots the perturbed data with a white noise of 5%.

Please cite this article in press as: Jalocha, D., et al. Revisiting the identification of generalized Maxwell models from experimental results. Int. J. Solids Struct. (2015), http://dx.doi.org/10.1016/j.ijsolstr.2015.04.018

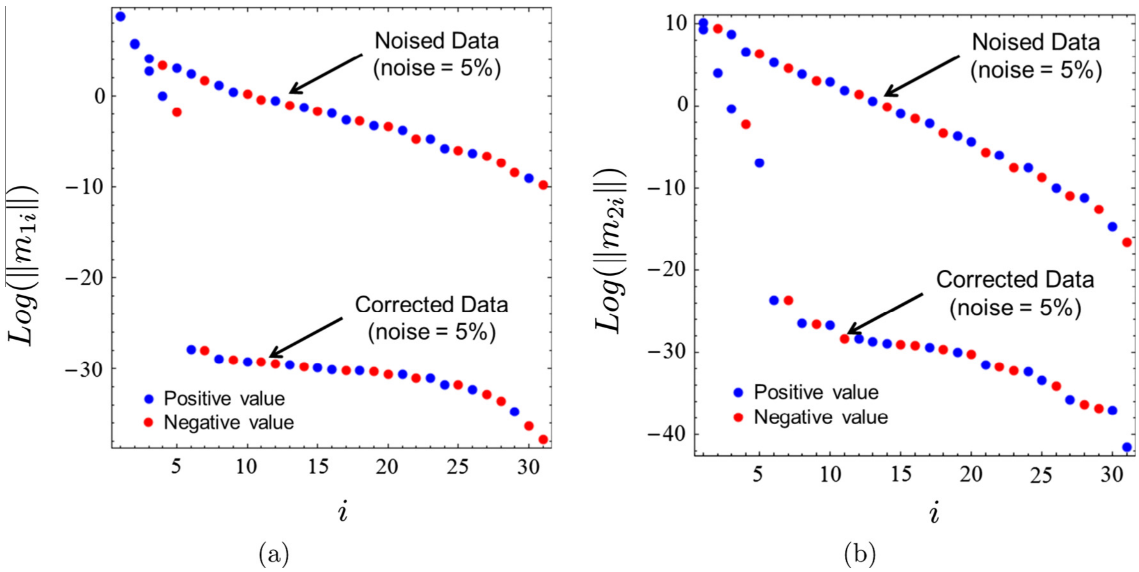

Fig. 4. Norm of the eigenvalues of the matrices M^1 and M^2 in panels (a) and (b) respectively. Each panel represents in a logarithmic scale the distribution of eigenvalues before and after the "correction" of the data. The color code displays positive eigenvalues in blue and negative ones in red. (For interpretation of the references to color in this figure legend, the reader is referred to the web version of this article.)

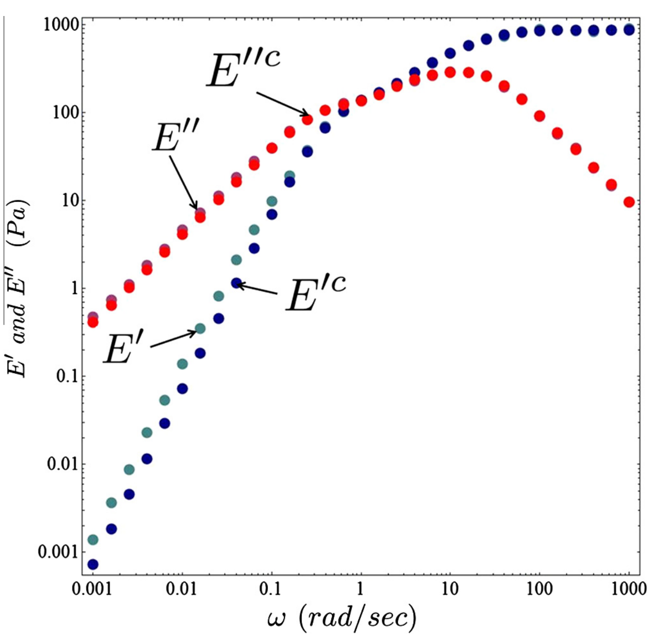

Fig. 5. The evolution of the real and imaginary part of complex modulus perturbed with 5% noise. E' and E'' represent the data before and E'^c and E''^c after "correction".

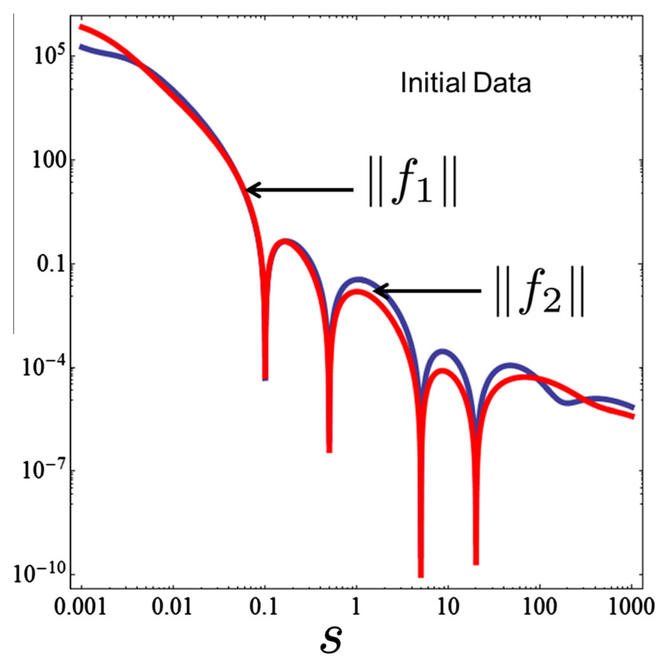

Fig. 6. Evolution of $\|f_1\|$ and $\|f_2\|$ as function of s computed with the initial unperturbed data.

The comparison between the data and the predicted evolution of the real part and imaginary part of the complex modulus displayed in Fig. 9 shows that both methods, HW and HW + KN, present an excellent match with the initial data. However, one should keep in mind that the HW + KN method used only 3 elements compared with the 6 elements corresponding to one for every time decade in the classical *HW* method. The result of the HW + KN method which determined directly the relaxation times was capable of predicting 3 out of the 4 relaxation times with the correct order of magnitude. The relative error is increasing with the value of the relaxation time and the long relaxation time is lost. However, the influence of noise up to 10% is small as the two noisy cases predicted very close results.

The capacity of the identified models to predict the relaxation modulus is presented in Fig. 10. The overall match is good for both methods, however for short relaxation times one obtains a better match with the KN + HW model in spite of having only 3 viscoelastic elements.

5.2. Parameter identification using the relaxation modulus

Let us now identify the same model from the artificial relaxation data and compare the results obtained from the *B* and *R* method.

Please cite this article in press as: Jalocha, D., et al. Revisiting the identification of generalized Maxwell models from experimental results. Int. J. Solids Struct. (2015), http://dx.doi.org/10.1016/j.ijsolstr.2015.04.018

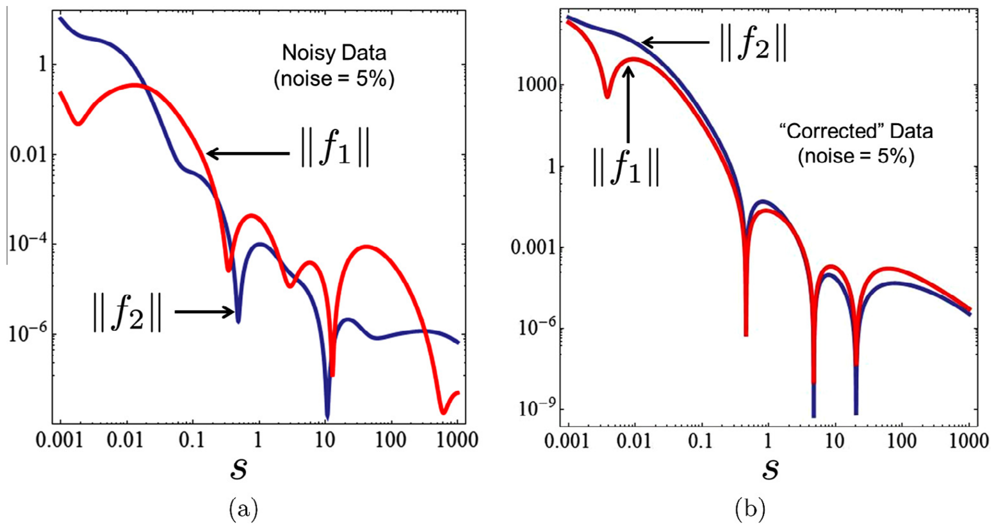

Fig. 7. Evolution of $\|f_1\|$ and $\|f_2\|$ in function of s for (a) the noised data (5%) and (b) the corrected data.

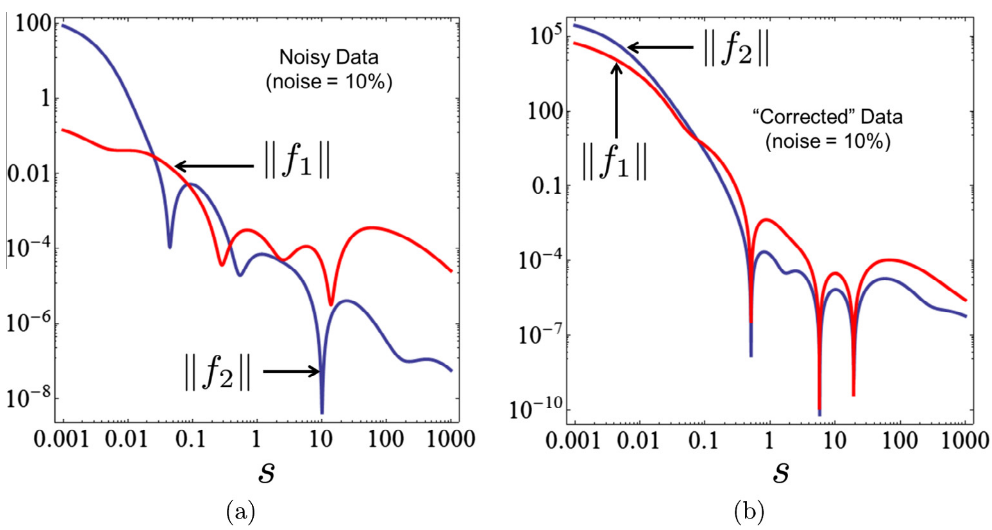

Fig. 8. Evolution of $\|f_1\|$ and $\|f_2\|$ in function of s for (a) the noised data (5%) and (b) the corrected data.

Table 3
Comparison of the identification results between the initial data, the HW method with 5% noise and the KN + HW method with 5% and 10% noise.

Initial data	τ_i (s)	0.05		0.2		2	10
	E_i (Pa)	400		300		150	8
HW method 5%	τ_i (s)	0.01	0.039	0.15	0.63	2.5	10
	E_i (Pa)	22.4	346.4	352.8	42.8	134.2	0.1
KN + HW method 5%	τ_i (s)	0.49		3.1		24.3	
	E_i (Pa)	465		275		116	
KN + HW method 10%	τ_i (s)	0.50		5.78		19.23	
	E_i (Pa)	459		271		119	

The identification of the expression of the relaxation modulus used in the preceding section, see Eq. (28), using a least square fit from the initial artificial data conducts to the following values of the parameters: $E_g = 850$ Pa, $E_0 = 0$ Pa, $t_0 = 0.094$ s and $\beta = 0.903$. The comparison between the data and the predictions of the formula are displayed in Fig. 11(a). In Fig. 11(b) we represent the evolution of the continuous spectrum H with respect to the time on a logarithmic scale, see also Eq. (31). The spectrum H reaches its maximum value of $H_{max} = 277$ Pa at $\tau = 0.104$ s. The support of the spectrum H will be defined as the interval situated between $\tau_{c1} = 0.008\, s \leqslant \tau \leqslant \tau_{c2} = 148\, s$, corresponding to $c_1 = 0.005$.

The R method computes the relaxation times using the minimization of the residual function R, given in Eq. (34). Using the identified models for an increasing number of viscoelastic elements in the generalized Maxwell model, $n = 1,\ 12$ in this example, one can also estimate the optimal number of viscoelastic elements n. We recall that the generalized Maxwell model represents a discrete spectrum $\hat{H}$ which is an approximation of the continuous spectrum H. The minimization of the residual function R was performed using standard Mathematica (Wolfram Research, 2014) operators with a final precision corresponding to a 1% relative error. The value of the residual R as a function of the number of viscoelastic elements n of the model is plotted in Fig. 12. A reasonable compromise between model prediction and number of

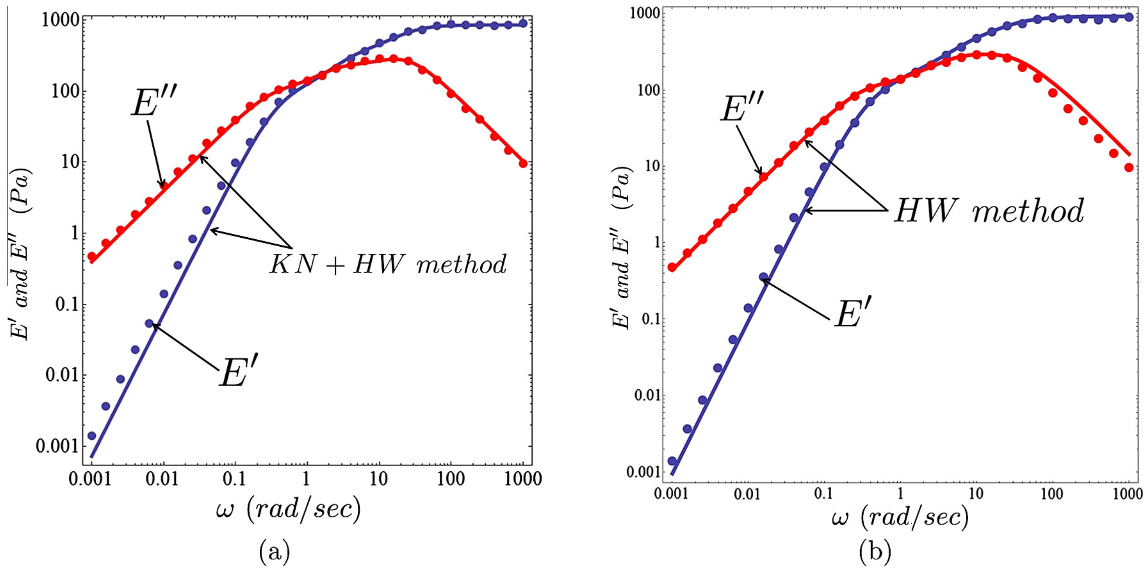

Fig. 9. Comparison for the complex modulus of the perturbed data with 5% noise (points) with the identified generalized Maxwell model (continuous line): on panel (a) *KN + HW method* with 3 elements (KN relaxation times), on panel (b) *HW method* with 6 elements (equidistantly distributed relaxation time on the logarithmic time axis) (Material parameters from Table 3).

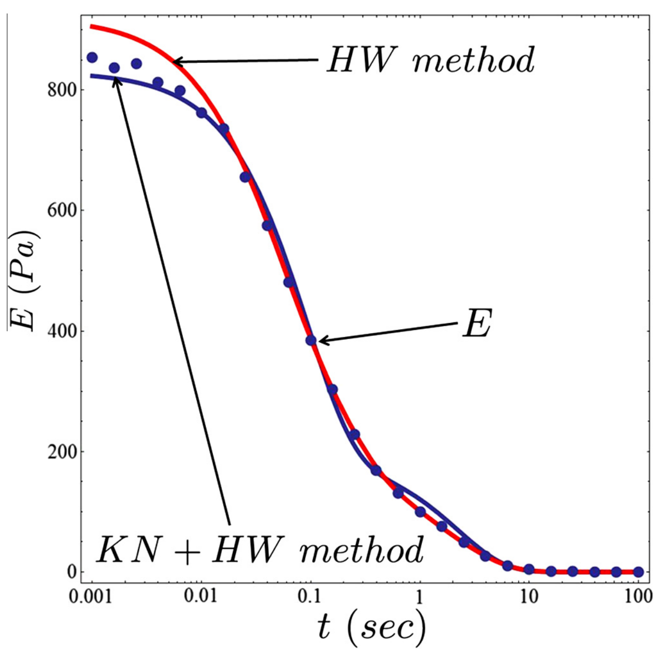

Fig. 10. Comparison of the predictions of the relaxation modulus obtained with the initial model *E*, the HW method with 5% noise and HW + KN method with 5% noise, models identified using DMA data (Material parameters from Table 3).

elements is already obtained with $n = 5$ elements. The values of the identified model parameters for $n = 5$ are given in Table 4.

For comparison we have also performed a complete identification of a generalized Maxwell model associated to this continuous relaxation using the B method, see (32). The best result was obtained using a discretization of the time interval $(10^{-3}\,s, 10^{3}\,s)$ with 9 discrete values placed at equal distances on logarithm scale. The final values of the identified parameters are displayed in Table 4.

The comparison between the prediction of the relaxation modulus and real and imaginary part of the complex modulus given by different models obtained with the R and B method are displayed in Fig. 13. The predictions of the relaxation modulus, see Fig. 13(a), show that a model with optimal relaxation times (method R) with 5 elements matches the data with the same accuracy as a model with logarithmic distributed relaxation times and 9 elements, B method. Moreover, if the number of elements is also reduced to 5 elements in the case of logarithmic distributed relaxation times, B method, the results are far from satisfactory.

The predictions of the complex modulus obtained using the same models, see Fig. 13(b), show that both method proved a good match for medium and high pulsations. However only the model with optimal relaxation times, the R method, matches the data for small pulsations, in spite of the apparent good match of both models for the relaxation modulus.

We can conclude the discussion of the examples using artificial data by stating that the generalized Maxwell model identified with optimal relaxation times, either using the complex modulus obtained by DMA experiments with the HW + KN method or using the relaxation modulus with the R method have almost half the number of viscoelastic elements of models identified using a logarithmic distribution of relaxation times for a similar accuracy.

6. Application to experimental results

As a second application of the methods we shall consider experimental data for the complex modulus of Polycarbonate and relaxation data for Asphalt from literature (Park and Kim, 2001).

6.1. Parameter identification using the complex modulus

The measurements have been performed using Dynamical Mechanical Analysis on Polycarbonate (PC). The complex modulus of PC is given for a reference temperature of 140 °C. A circular disk of PC, 2 mm of height and 25 mm of diameter, is submitted to a torsional DMA test using an ARES rheometer for a frequency range between 10^{-3} and 10 rad/s.

The identification results obtained using the KN + HW method following the steps described before. The common zeros of the functions indicates 5 relaxation times. The values of the identified

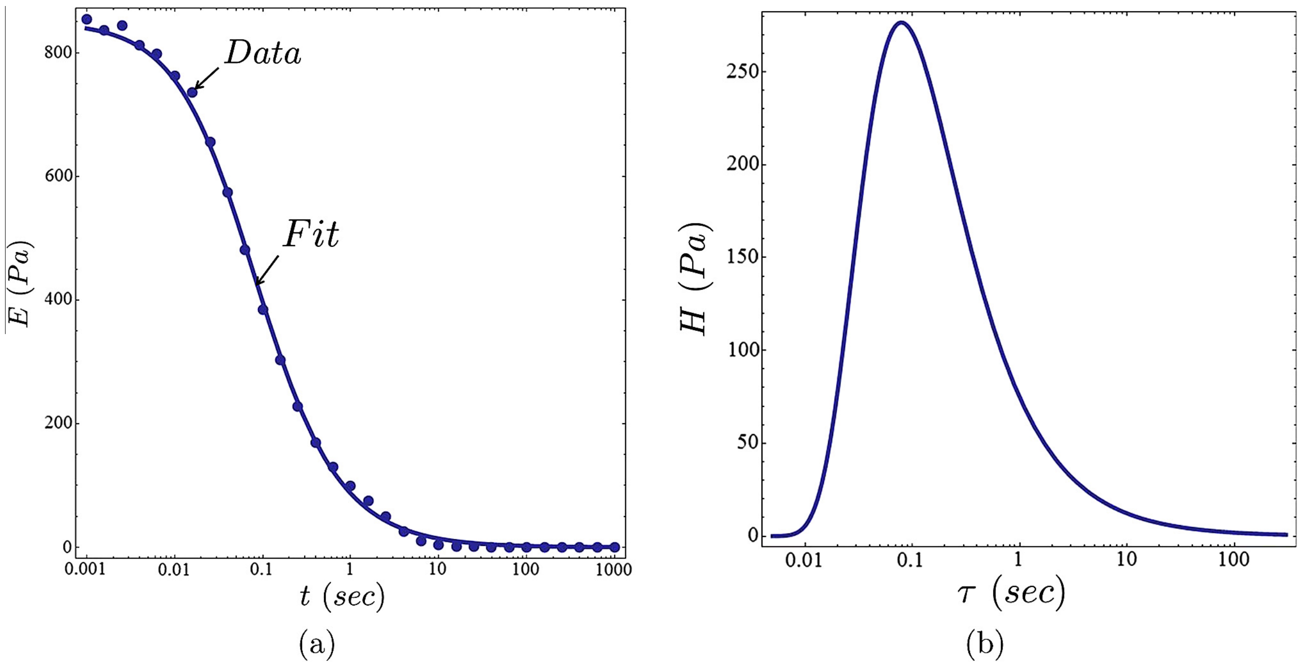

Fig. 11. (a) Fitted relaxation modulus using Eq. (28) ($E_g = 850$ Pa, $E_0 = 0$ Pa, $t_0 = 0.094$ s and $\beta = 0.903$). (b) Continuous spectrum computed from the relaxation modulus.

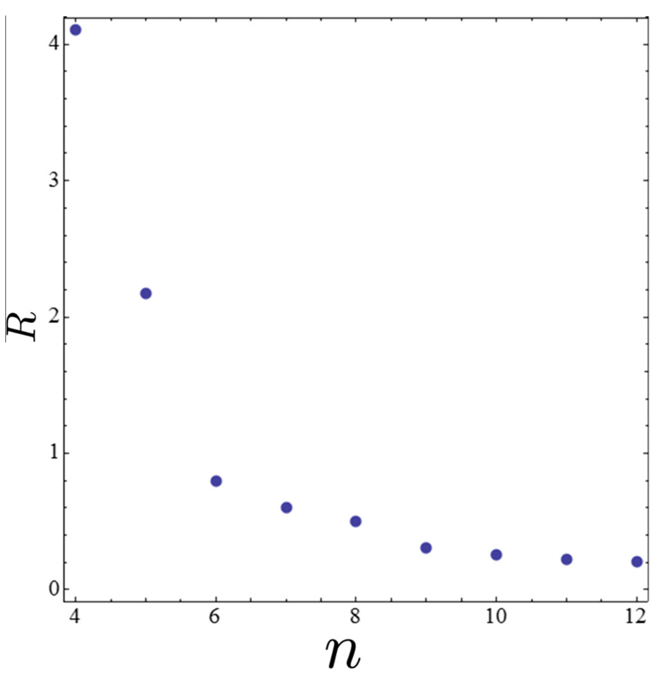

Fig. 12. Evolution of the residual function R (34) with respect to the number of viscoelastic elements n in the optimal generalized Maxwell model.

material parameters of the optimal generalized Maxwell model with 5 elements are given in Table 5. For comparison reasons we have equally identified a model with 5 elements using the HW method and the values of the parameters are also given in Table 5. The comparison of the real and imaginary part of the complex modulus is presented in Fig. 14. Panel (a) represent the KN + HW method and panel (b) represents the HW method. An inspection of the plots shows that for the same number of viscoelastic elements only the model identified using optimal relaxation times is capable to match the data. It also shows that 4 decades of pulsation are accurately represented using 5 viscoelastic elements.

6.2. Parameter identification using the relaxation modulus

The experimental data for the relaxation modulus of the Asphalt Concrete at 25 °C has been recovered from literature (Park and Kim, 2001).

The first step in the identification process was the identification of the relaxation modulus E given by the closed form expression of Eq. (28) from the data and the computation of the relaxation spectrum H, Eq. (31). The coefficients are $E_0 = 0$, $E_g = 12450$ MPa, $t_0 = 1.4\ 10^{-4}$ s and $\beta = 0.39$.

The second step consist in identifying the parameters of the generalized Maxwell model. First the R method is applied for $c_1 = 0.005$. The results provide a good fit for only $n = 6$ viscoelastic elements in the generalized Maxwell model. Second, for

Table 4
Comparison with initial of the identification results for the relaxation experiments using B method with 5% noise and $n = 9$ elements and the R method with 5% and 10% noise and $n = 5$ elements.

Initial data	τ_i (s)			0.05	0.2	2		10		
	E_i (Pa)			400	300	150		8		
B method 5%	τ_i (s)	0.001	0.005	0.03	0.17	1	5.6	31.6	177	1000
	E_i (Pa)	$3\ 10^{-24}$	0.1	298	388	128	33	8	2	0.25
R method 5%	τ_i (s)		0.016	0.06	0.2	0.78		9.8		
	E_i (Pa)		52	434	194	120		45		
R method 10%	τ_i (s)		0.016	0.061	0.2	0.79		9.81		
	E_i (Pa)		52	435	195	121		45		

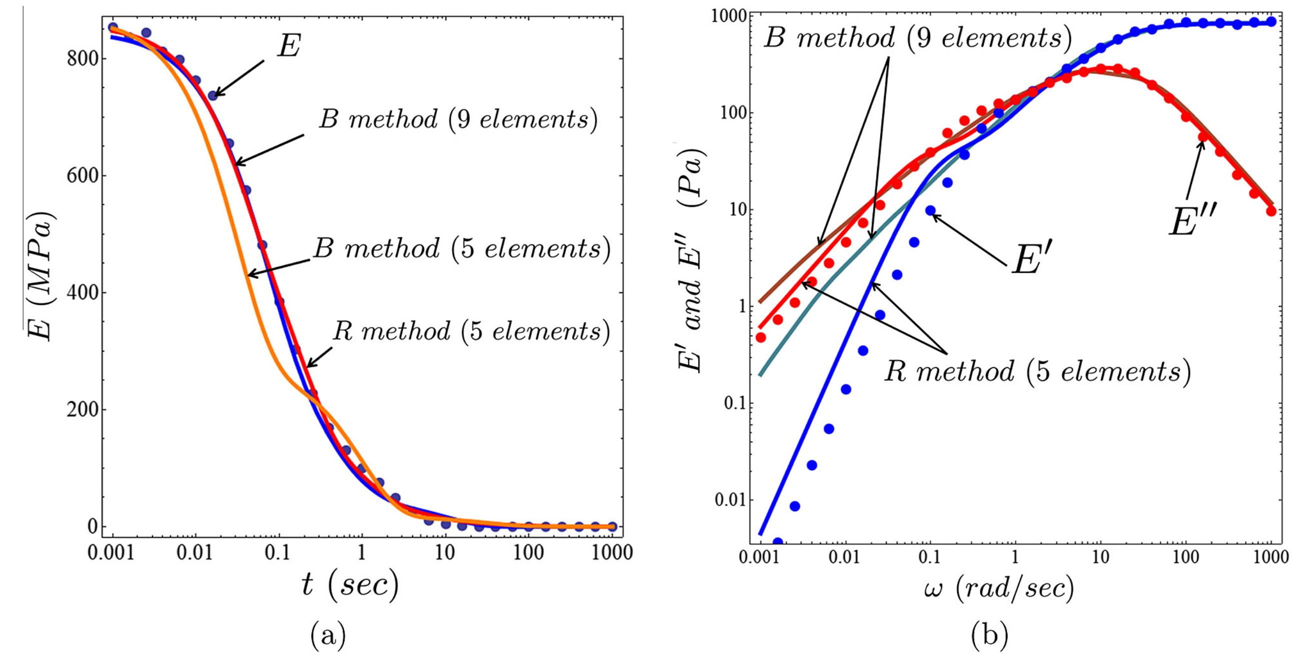

Fig. 13. (a) Relaxation modulus data, with the predicted generalized Maxwell model given by the B method and the R method (Table 4). (b) Complex modulus data, with the predicted complex modulus given by "B method" and "R method" (Table 4).

Table 5
KN + HW method for the PC complex modulus data

HW method	τ_i (s)	0.1	1	10	100	1 000
	E_i (Pa)	4.4 10^7	9.5 10^7	1.8 10^8	2.1 10^8	2.3 10^7
KN + HW method	τ_i (s)	0.23	0.83	5.5	38.4	251
	E_i (Pa)	5.1 10^7	6.1 10^7	1.2 10^8	1.9 10^8	9.6 10^7

comparison, a model is also identified using the B method. The identified coefficients are reported in Table 6 for both models.

The comparison of the predictions of the relaxation modulus are exhibited in Fig. 15. As before, for the same number of elements, $n = 6$ in this case, the R method, using optimal relaxation times provides a very good match with the experimental data of the relaxation modulus. The B method provides only a rough estimate at short relaxation times, where the modulus is overestimated and an oscillating with important errors for medium times. Additional computations have shown that the B method needs at least $n = 12$ viscoelastic elements to match the experimental relaxation data with the same accuracy as the R method with $n = 6$ elements.

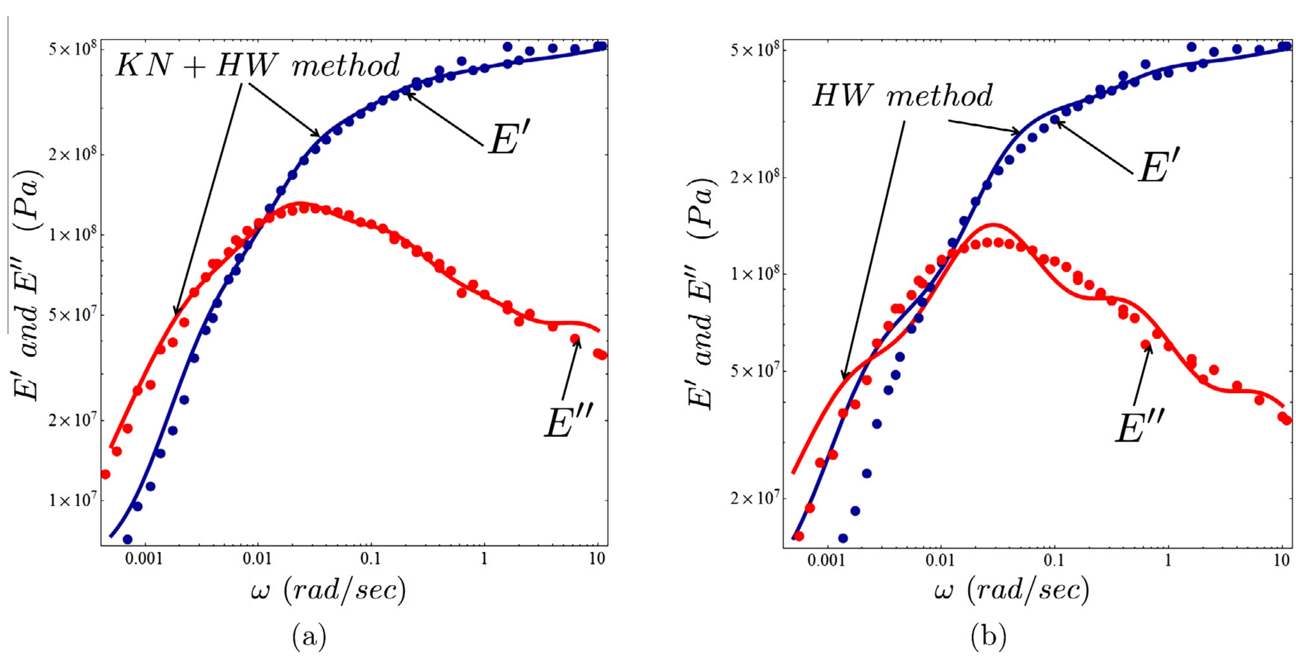

Fig. 14. Complex modulus of PC predicted using a 5 elements generalized Maxwell model identified with (a) the *KN + HW method* and (b) the *HW method*. The coefficients of the model are given in (see Table 5).

Table 6
Identified coefficients using the *R* and *B method* for the relaxation modulus of Asphalt Concrete (experimental data from Park and Kim (2001)).

B method	τ_i (s)	2.3 10^{-6}	4.1 10^{-4}	6.7 10^{-2}	11.3	322	1913
	E_i (MPa)	1.3 10^{-7}	13.1 10^{3}	2.4 10^{3}	329	43.5	2.8
R method	τ_i (s)	1 10^{-4}	9 10^{-4}	6 10^{-3}	4.3 10^{-2}	0.38	1.53
	E_i (MPa)	4 10^{3}	4.3 10^{3}	2.2 10^{3}	1.6 10^{3}	5.7 10^{2}	62.29

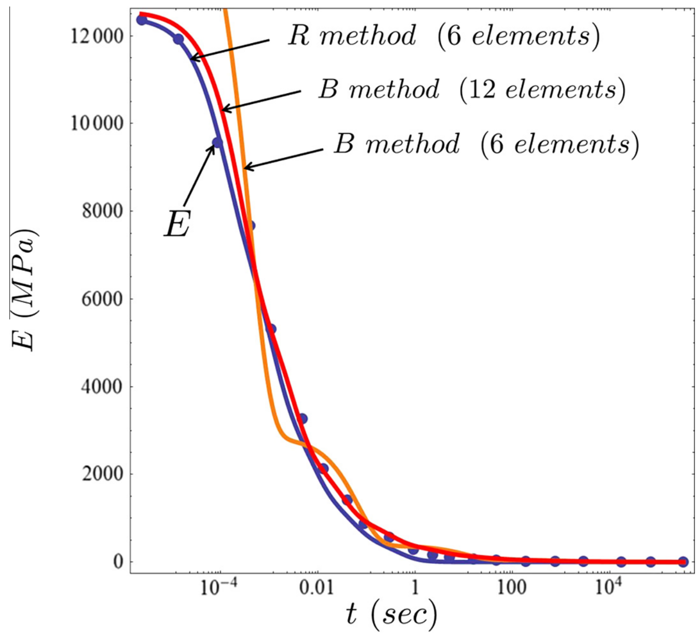

Fig. 15. Comparison of the prediction of the relaxation modulus of Asphalt Concrete (data from Park and Kim (2001)) using the *R* and *B method* with $n = 6$ and 12 elements in the generalized Maxwell model.

7. Conclusion

This paper discussed the identification of the material parameters of a generalized Maxwell model in linear viscoelasticity. The parameters of the model are determined either from the relaxation modulus or from the dynamic modulus obtained from either relaxation or a DMA experiment respectively.

The focus of the discussion was the choice of the characteristic relaxation times representing the viscoelastic elements of the models. The standard identification methods presented in literature rely generally on an a priori chosen discrete series of relaxation times, often taken as a logarithmic distribution over an interval. Fixing the relaxation times in advance of the main process permits to both simplify and regularize the ill-posed character of the identification procedure.

The paper presented improvements of the methods by proposing alternative methods for the choice of the relaxation times: (i) using the Krein Nudelman theorem from complex analysis to determine the exact relaxation times as zeros of complex functions in the case of the complex modulus and (ii) minimizing of the relative distance between the discrete approximation and the continuous relaxation spectrum measured using a Riemann integral in the case of the relaxation modulus. The key-point of both methods is their capacity to provide a stable and precise way to estimate a discrete series of relaxation times. These modifications demand only several additional matrix computations and minimization when compared with the traditional identification procedures. These operations are current operators in general purpose programs like Mathematica, Matlab, etc. The identification process for the examples discussed in the paper takes several seconds on a standard laptop and are therefore not an additional numerical difficulty.

The methods have been applied to both artificial data with and without noise and to experimental data. In all discussed examples the generalized Maxwell models identified with optimal relaxation times had half the number of viscoelastic elements of models as models using a logarithmic distribution of relaxation times for a similar accuracy. Moreover using optimal relaxation times provided models with a better cross predication of data, i.e. prediction of relaxation modulus with a model identified on the complex modulus or conversely.

This work opens new perspectives in the determination of nonlinear generalized Maxwell models when the elastic moduli of the viscoelastic elements will depend also on additional parameters such a temperature, prestrain, etc. In this cases an optimal distribution of relaxation times proves to be key element in the stability and accuracy of the identified model.

Acknowledgments

The authors would like to thank the French Direction Generale de l'Armement, Laurent Munier (DGA) and HERAKLES-SAFRAN for financial support.

References

Baumgaertel, M., Winter, H., 1992. Interrelation between continuous and discrete relaxation time spectra. J. Non-Newtonian Fluid Mech. 44, 15–36.
Brinson, C., 2008. Polymer Engineering Science and Viscoelasticity. An Introduction.
Buhanand, M., Osses, A., 2010. Logarithmic stability in determination of a 3D viscoelastic coefficient and a numerical example. Inverse Prob. 26, 1088–1112.

Byrnes, C., Lindquist, A., 2000. On the duality between filtering and Nevanlinna–Pick interpolation. Soc. Indust. Appl. Math. 39, 757–775.

Carrot, C., Verney, V., 1996. Determination of discrete relaxation spectrum from dynamic experimental data using the Pade Laplace method. Eur. Polym. J. 32, 69–77.

Cavaterra, C., Grasselli, M., 1997. On an inverse problem for a model of linear viscoelastic Kirchhoff plate. J. Integral Equ. Appl. 9, 179–218.

Collet, P., Gary, G., Lundberg, B., 2013. Noise-corrected estimation of complex modulus in accord with causality and thermodynamics: application to an impact test. J. Appl. Mech. 80 (1).

Diani, J., Gilormini, P., Fredy, C., Rousseau, I., 2012. Predicting thermal shape memory of crosslinked polymer networks from linear viscoelasticity. Int. J. Solids Struct. 49, 793–799.

Findley, W., Lai, J., Onaran, K., 1976. Creep and Relaxation of Nonlinear Viscoelastic Materials.

Gerlach, S., Matzenmiller, A., 2005. Comparison of numerical methods for identification of viscoelastic line spectra from static test data. Int. J. Numer. Meth. Eng. 63, 428–454.

Grasselli, M., 1994. Determining the relaxation tensor in linear viscoelasticity of integral type. Jpn. J. Indust. Appl. Math. 11, 13153.

Greene, R., Krantz, S., 1997. Function Theory of One Complex Variable. John Wiley and Sons.

Gu, G., Xiong, D., Zhou, K., 1993. Identification in h using Pick's interpolation. Syst. Control Lett. 20, 263–272.

Hansen, P.C., 1992. Numerical tools for analysis and solution of Fredholm integral equations of the first kind. Inverse Prob. 8 (6), 849.

Honerkamp, J., 1989. Illposed problems in rheology. Rheol. Acta 28, 363–371.

Honerkamp, J., Weese, J., 1990. Tikhonovs regularization method for ill-posed problems. Cont. Mech. Thermodyn. 2, 1730.

Janno, J., Von Wolfersdorf, L., 1997. Inverse problems for identification of memory kernels in viscoelasticity. Math. Meth. Appl. Sci. 20, 291–314.

Krein, M., Nudelman, A., 1998. An interpolation problem in the class of Stieltjes functions and its connection with other problems. Integr. Eqn. Oper. Theory 30, 251–278.

Kurtz, D., Kurweil, J., Swartz, C., 2004. Theory of Integration. Scientific Publishing Co., Pte. Ltd.

Lavrentiev, M., 1967. Some Ill-Posed Problems of Mathematics Physics. Springer, Berlin.

Lorenzi, A., 1999. A multidimensional identification problem related to a hyperbolic integrodifferential equation. Z. Anal. und ihre Anwendungen 18, 407–435.

Lorenzi, A., Romanov, V., 2006. Stability estimates for an inverse problem related to viscoelastic media. J. Inverse Ill-Posed Prob. 18, 407–435.

Markovitz, Hershel, 1977. Boltzmann and the beginnings of rheology. Trans. Soc. Rheol. 21 (3), 381–398.

Otegui, J., Ramos, J., Vega, J.F., Martnez-Salazar, J., 2013. Effect of high molar mass species on linear viscoelastic properties of polyethylene melts. Eur. Polym. J. 49, 2748–2758.

Park, S., Kim, Y., 2001. Fitting prony-series viscoelastic models with power-law presmoothing. J. Mater. Civil Eng. 13, 26–32.

Press, H., Teukolsky, A., Vetterling, T., Flannery, P. Numerical recipes, The art of Scientific Computing.

Simo, J.C., Hughes, T.J.R., 2008. Computational Inelasticity. Springer.

Smith, T., 1971. Empirical equations for representing viscoelastic functions and for deriving spectra. J. Polym. Sci. 35, 39–50.

Thorin, A., Azoug, A., Constantinescu, A., 2013. Influence of prestrain on mechanical properties of highly-filled elastomers: measurements and modeling. Polym. Testing 31, 978–986. http://dx.doi.org/10.1016/j.polymertesting.2012.07.014.

Thorin, A., Azoug, A., Neviere, R., Constantinescu, A., Praidelles-Duval, 2013. Influence of orthogonal prestrain on the viscoelastic properties of highly-filled elastomers: measurements and modeling. Polym. Testing 32 (8). http://dx.doi.org/10.1016/j.polymertesting.2012.12.005.

Von Wolfersdorf, L., 1993. On identification of memory kernels in linear viscoelasticity. Mathematische Nachriten 161, 203–217.

Widder, D., 1946. The Laplace Transform. Princeton University Press.

Wolfram Research Inc. Mathematica, Version 10.0, Champaign. IL, USA. 2014.

Xiao, R., Choi, J., Lakhera, N., Yakacki, C., Frick, C., Nguyen, T., 2013. Modeling the glass transition of amorphous networks for shape memory behavior. J. Mech. Phys. Solids 61, 1612–1635.

Zarrelli, M., Skordos, A., Partridge, K. Toward a constitutive model for cure-dependent modulus of a high temperature epoxy during the cure. Eur. Polym. J. 46 (1705–1712), 46.

Please cite this article in press as: Jalocha, D., et al. Revisiting the identification of generalized Maxwell models from experimental results. Int. J. Solids Struct. (2015), http://dx.doi.org/10.1016/j.ijsolstr.2015.04.018